

# Stirrers and movers actuated by oscillating fields

Gabi Steinbach,<sup>1,2</sup> Michael Schreiber,<sup>1</sup> Dennis Nissen,<sup>3</sup> Manfred Albrecht,<sup>3</sup> Sibylle Gemming,<sup>1,2</sup> and Artur Erbe<sup>2</sup>

<sup>1</sup>*Institute of Physics, Technische Universität Chemnitz, D-09107 Chemnitz, Germany.*

<sup>2</sup>*Helmholtz-Zentrum Dresden-Rossendorf, Institute of Ion Beam Physics and Materials Research, Bautzner Landstrasse 400, 01328 Dresden, Germany.*

<sup>3</sup>*Institute of Physics, University of Augsburg, 86159 Augsburg, Germany.*

We present a concept for the actuation of structurally non-deforming objects under oscillating fields in a highly viscous environment, a process which so far is considered impossible. The objects are self-assembled clusters of colloidal particles that are held together solely by magnetic forces. Based on analytic and numerical studies, we demonstrate that an oscillating field, which induces only reciprocal motion on a single, rigid particle, can propel such clusters if the composing particles exhibit an off-centered dipole moment. This unexpected observation can be understood when taking into account that the magnetic interaction between such particles in the cluster breaks time-reversal symmetry under oscillating fields. We approve this theoretical prediction with an experimental system of magnetic Janus particles, and show that the magnetic configuration of a cluster of such Janus particles determines its motion path. It can range from rotation to helical motion and directed translation, where the orientation of the latter can be controlled by an additional constant, weak magnetic field. The presented concept establishes a counterpart to the actuation of deforming objects, such as artificial flagella, in oscillating fields, and to motion in rotating fields.

Since Purcell proposed the Scallop theorem in 1977 [1], locomotion of microscopic objects has been the subject of intense research [2–6]. The fascination for migration at this length scale arises from the time reversibility of motion patterns in highly viscous environments, where inertia can be neglected. In many everyday cases such as swimming, locomotion is generated by a cyclic process; in such cases this time reversibility limits the possibility of migration. Under any oscillating pattern of motion, a rigid microscopic object repeatedly goes back and forth by the same distance. Such a so-called reciprocal motion excludes directed migration. Yet, nature has found ways for microorganisms to move [7–14]. Typically, these organisms exploit anisotropic drag to break time reversibility. Beyond that, artificial propulsion methods have been established based on controlled shape changes or changes in the chemical environment of the objects [15–23]. The aim is to improve the control over translation patterns and to increase the choice of materials/environments for advanced applications in non-invasive medicine and lab-on-chip systems.

Torque-based magnetic actuation, i.e. propulsion of magnetic micro-objects via their alignment in time-dependent fields, is particularly advantageous [23–27]. It can be controlled remotely, only homogeneous fields are required, and it is widely independent from the chemical environment and the optical properties of the system. Since a torque causes a magnetic moment to solely rotate by an angle  $\theta$ , translation  $r$  can be induced only if the rotation creates a force on the center of mass of the object.

To date, most examples of magnetic actuation exploit hydrodynamic coupling between rotation and translation [23, 27]. There, coupling appears if the object has a helical shape (propelling) [28–30], or if the environment is

anisotropic, e.g., close to a no-slip surface (rolling) [31–33] (Fig. 1 A). However, under any cyclic, torque-based actuation this coupling leads to an effective displacement only if the start- and the endpoint of each cycle differ. Due to time reversibility, this can be realized only if at least two coordinates of motion of the object are affected in a time-dependent manner. Trivially, this is the case under rotating or precessing fields, which act along two coordinates (Fig. 1 C), and lead to rolling or propelling [23, 28, 30, 34]. In contrast, an oscillating field exerts a time-dependent torque along one coordinate only, leading to reversibly back and forth motion of a rigid object between maximum deflection angles  $\pm\theta_A$ . In terms of applications, oscillating fields are, however, advantageous over rotating fields since technically they are much easier to generate and to exert on a sample. The challenge is, thus, to activate motion along an additional coordinate that breaks time reversibility. So far, this has been realized only by incorporating structural flexibility. Reported systems comprise objects with flexible tails

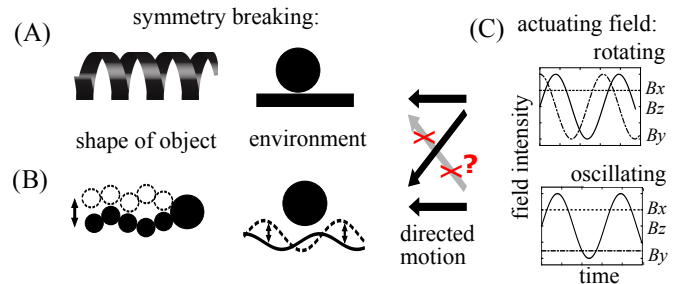


FIG. 1. Overview over concepts for magnetic actuation through anisotropic drag. Types of symmetry breaking (A) of rigid systems and (B) of flexible systems, and (C) actuating fields.

(Fig. 1 B), resembling flagella [35–37]. During the field oscillation they perform asymmetric undulations, and the hydrodynamic coupling leads to propulsion. Also, rigid objects can be actuated in the proximity of an elastic (flexible) surface [38].

Here, we present an alternative actuation concept that enables the propulsion of structurally non-deforming objects with oscillating fields. The studied objects are self-assembled clusters of a few spheres that exhibit an off-centered net magnetic moment. The additional mobility is given by the fact that the individual spheres are able to rotate inside the cluster. The relative distances between all spheres within a cluster remain constant, hence these are non-deforming clusters. We explain the concept qualitatively with a simple theoretical model. It assumes spheres with an embedded dipole that is not centered but shifted radially outwards, so-called shifted-dipole particles (sd-particles). The interaction of the spheres with this magnetic asymmetry breaks time-reversal symmetry under oscillating fields, causing motion even without the need for hydrodynamic drag. The theoretical predictions can be verified with an experimental system of magnetic Janus spheres. Experimentally, we obtain a variety of motion paths, which depend on the cluster configuration.

## RESULTS

The actuation concept consists of two elements. First, the conversion of rotation into time-reversible translation is achieved by each particle separately, hence, a single-particle problem. Second, the breaking of the time reversibility arises from the interaction between the particles in a cluster. In the following, these two elements are demonstrated qualitatively by a combination of analytic and numerical calculations with sd-particles. Afterwards, the investigations are used to explain our experimental observations of actuated clusters from spheres with a hemispherical magnetic coating, which move under oscillating fields.

### Analytic expression for the oscillation of single sd-particles

We assess the role of magnetic asymmetry of a single dipolar particle by considering its reciprocal motion under oscillating fields for four different scenarios (Fig. 2). If, in an isotropic medium, a sphere with a central dipole (case i, Fig. 2) is exposed to an oscillating field  $B^z = B_0^z \sin(\omega_B t)$ , the dipole follows the field via up and down rotation by angle  $\theta \in [-\theta_A, \theta_A]$ . As a magnetic object rotates around its magnetic center this results only in particle rotation. Asymmetry is introduced by sd-particles, where the magnetic center is shifted away from the geometric center (case ii, Fig. 2). Here, the dipole is

shifted radially outwards by  $\xi \frac{d_p}{2}$  along the dipole orientation, where  $\xi \in [0, 1]$  is the shift parameter and  $d_p$  is the particle diameter. Under oscillating fields, the rotation around the magnetic center displaces the particle center periodically. In an isotropic environment, the particle center moves on an arc [39] with a radius determined by the shift  $\xi$ . The behavior changes in the proximity of a wall, where anisotropic drag is present. We consider this case here because the experiments described later in this work are performed on particles moving close to a planar substrate. We emphasize that the presence of a wall is, however, not essential for the actuation mechanism presented here.

Already for a sphere with central dipole (case iii, Fig. 2) in a liquid medium close to a wall, rotation is converted into reversible back and forth displacement. An sd-particle also rolls back and forth, and additionally performs a periodic displacement away from the wall and towards the wall (case iv, Fig. 2) because the magnetic center is shifted away from the geometric center of the sphere. In contrast to case iii, this motion is not symmetric with respect to  $\theta$  due to the hindrance by the wall.

For an sd-particle in an isotropic medium, we can derive an analytic expression for the displacement of the particle center that arises from the rotation by an infinitesimal angle  $d\theta$  around the magnetic center (see Appendix). The infinitesimal displacement, separated into components perpendicular ( $dr$ ) and parallel ( $dz$ ) to the oscillating field  $B^z$ , is given by

$$dr = -\xi \frac{d_p}{2} c(\theta) \sin \theta d\theta, \quad (1a)$$

$$dz = \xi \frac{d_p}{2} c(\theta) \cos \theta d\theta. \quad (1b)$$

The term  $c(\theta)$  contains potential sources of anisotropy

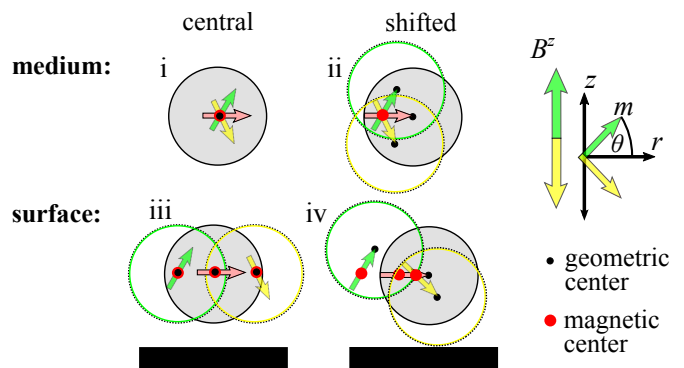


FIG. 2. Time-reversible motion of a single dipolar sphere under oscillating magnetic fields  $B^z$ . The scenarios depict a sphere with central dipole (i, iii) and shifted dipole (ii, iv) in an isotropic medium (i, ii) and close to a wall (iii, iv). The dipole (light red arrow) with moment  $m$  oscillates up (green) and down (yellow) which results in a displacement of the sphere (dotted green and yellow circles) under asymmetric conditions (ii-iv).

hindrance or enhancement. For a single particle, this is given by, e.g., a wall. The determination of  $c(\theta)$  close to a wall is a complex problem. Since the rotation around the shifted magnetic center periodically changes the distance between particle center and wall, also the hydrodynamic friction coefficient changes periodically. To illustrate the concept, here, it is sufficient to approximate the surface-induced drag with a step function of two values  $c_1, c_2$  that alternate with the sign of  $\theta$ . Distinguishing between translation parallel ( $r$ ) and perpendicular ( $z$ ) to the surface gives

$$c_r(\theta) = \begin{cases} c_{r,1} & \text{if } \theta \geq 0 \\ c_{r,2} & \text{if } \theta < 0 \end{cases}, \quad c_z(\theta) = \begin{cases} c_{z,1} & \text{if } \theta \geq 0 \\ c_{z,2} & \text{if } \theta < 0 \end{cases}. \quad (2)$$

During  $\theta > 0$  (green circle in case iv, Fig. 2) the surface-induced translation (ii) enhances the translation  $r$  caused by the off-centered dipole (iii). During  $\theta < 0$  (yellow circle), the directions of the two translations are opposite to each other as can be seen by the comparison between cases ii and iii. Therefore, for oscillations close to a wall (iv) the displacement during  $\theta > 0$  is always higher than during  $\theta < 0$  and, thus,  $|c_1| > |c_2|$ . If the influence of the surface on the displacement is stronger than that of the shifted magnetic center, then during  $\theta < 0$  the overall translation direction is even inverted with respect to the one in an isotropic medium (ii), and  $c_{r,2} < 0$ . Otherwise  $c_{r,2} > 0$  holds. Note that the integral of Eq. 4 over one oscillation cycle ( $\theta = 0 \rightarrow \theta_A \rightarrow 0 \rightarrow -\theta_A \rightarrow 0$ ) becomes zero due to the time reversibility.

### Sd-particles in a ring cluster

Next, we transfer the considerations for a single sd-particle to sd-particles that form a two-dimensional cluster in the plane  $z = 0$ . We assume that within the cluster the particles are free to rotate in response to magnetic stimuli but that the relative distances between all particles are kept constant during field exposure. The simplest case to study interacting sd-particles is given if they form a ring. Then, ideally all particles have identical boundary conditions and behave uniformly. As an example, a ring of three particles (triple ring, Fig. 3 A) will be studied.

In analogy to a single sd-particle, rotation by  $d\theta$  displaces each sd-particle by  $dr$  and  $dz$ . However, since the particles are constrained to a circle (Fig. 3 A) and move uniformly, the displacement  $dr$  is forced along an orbit spanned by the particle centers. As a consequence, the displacement of each sd-particle, induced by the rotation  $d\theta$ , is hindered sterically by the presence of neighboring particles. The hindrance depends on the angle  $\varphi$  that is enclosed by the tangent to that orbit and the in-plane component of the dipole (Fig. 3 A).  $dr$  becomes zero if  $\varphi = 90^\circ$ , and it is completely unobstructed if  $\varphi = 0^\circ$ . Such an anisotropic hindrance is taken into account by

introducing the reduction factor  $c_f(\theta) = \cos \varphi(\theta)$ . This hindrance indirectly affects also the displacement  $dz$ .

The factor  $c_f(\theta)$  suggests that the hindrance between interacting particles depends exclusively on  $\varphi$ . To determine  $\varphi$  during the driven oscillations of sd-particles in a triple ring, we have studied the rotational (angular) motion of the particles separately from their translational motion. The rotational motion  $\varphi(\theta(t))$  has been obtained by numerically solving the equation of rotation of the interacting sd-particles under an oscillating field  $B^z$ , which points perpendicular to the plane of the ring cluster.

The periodic variation of  $B^z$  leads to an oscillatory behaviour of  $\theta(t)$ . Additionally, we have observed that the variation of  $\theta$  involves a periodic change of  $\varphi$  for interacting sd-particles in a ring. The trajectories of the dipoles in  $\theta$ - $\varphi$  coordinates are double loops (Fig. 3 B). Starting from the field-free equilibrium state (0), the dipoles perform a short transient oscillation until they reach a steady-state oscillation along the path I  $\rightarrow$  IV. The loop implies that the dipoles obtain larger angles  $\varphi$  while  $|\theta|$  increases (I/III) than during the part of the trajectory in which  $|\theta|$  decreases (II/IV) (Fig. 3 C). Such a loop trajectory  $\varphi(\theta)$  breaks time reversibility since the sense of direction of the loop is uniquely defined. Inserting  $\varphi(\theta)$  into the reduction term  $c_f(\theta) = \cos \varphi(\theta)$  gives rise to a time-irreversible translation of the sd-particles along the orbit. During increase of  $|\theta|$ , the displacement  $dr$  is hindered more strongly than during decrease of  $|\theta|$ . Based on that a non-reciprocal displacement  $dr$  of the sd-particles in the triple ring can be predicted, which leads to an effective rotation of the whole ring (Fig. 3 C).

Inserting the term  $c(\theta) = c_f(\theta) = \cos \varphi(\theta)$  into Eq. 4 gives the infinitesimal displacement of a particle in a ring located in an isotropic environment. The time dependence of the displacement  $dr(t)$  can be obtained by inserting analytic expressions for  $\varphi(\theta(t))$  and  $\theta(t)$ . Fitting the numerical data (Fig. 3 B) to Lissajous curves (see Appendix) yields suitable approximate functional terms. The net translation is obtained by integration,  $r(t') = \int_0^{t'} dr(t)$  (Fig. 3 D).

For a ring in an isotropic medium, the sd-particles periodically translate back and forth twice per movement cycle (Fig. 3 D) similar to a single particle (case ii, Fig. 2). In addition, they gain an overall distance  $\Delta r$  traveled after each movement cycle I  $\rightarrow$  IV. This is a very small effect since  $r$  is in the range of a few %  $d_p$ , and  $\Delta r$  is less than one tenth of that range.

The translation  $r(t)$  during one cycle can be detailed as follows. During increase of  $|\theta|$  (I/III), the particle translates with its magnetic side ahead (Fig. 3 C), defined as back motion. Forth translation with the non-magnetic side ahead occurs during sections II and IV. As derived from the rotational trajectory (Fig. 3 B), the factor  $\cos \varphi(\theta)$  during I/III is smaller than during II/IV. Therefore,  $-dr(\theta_I) = -dr(\theta_{III}) < dr(\theta_{II}) = dr(\theta_{IV})$ .

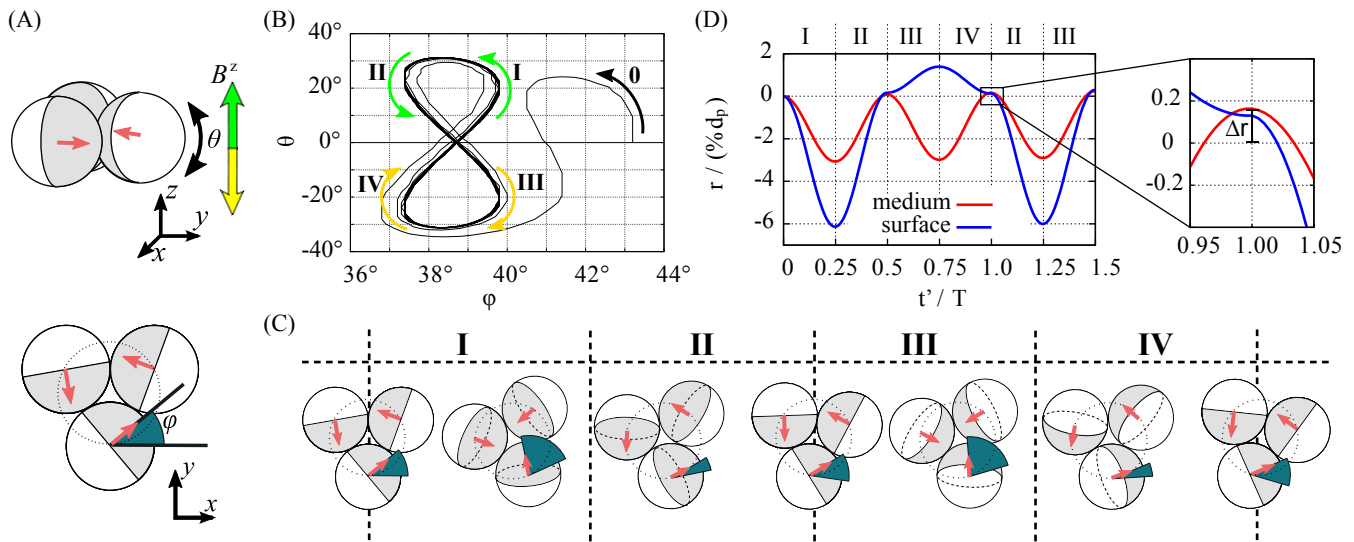


FIG. 3. Rotation of a ring of sd-particles. (A) Triple ring (side and top view), and orientation angles  $\varphi$  and  $\theta$  of sd-particles. For better visualization, the hemisphere that contains the dipole (red arrow) is colored in grey. The dotted ring indicates the orbit of motion spanned by the particle centers. (B) Numerically calculated trajectory in  $\theta - \varphi$  coordinates of an sd-particle ( $\xi = 0.55$ ) in a triple ring under an oscillating field ( $B_0^z = 6 \frac{\mu_0 m}{4\pi d_p^3}$ ). The arrows indicate the time evolution. (C) Sketched top view of a triple ring during one movement cycle. For clarity, the drawn variations in  $\varphi$  (green segments) are much larger than the ones plotted in (B). (D) Orbital translation  $r$  versus time  $t'$  of an sd-particle in a triple ring that is located in an isotropic medium or on a surface ( $c_1 = 2$  and  $c_2 = -0.4$ ). The time  $t'$  is measured in period  $T$ .

The integration of  $dr$  over one field cycle is, thus, positive. The particles in a ring perform a net translation along the orbit with the non-magnetic side facing forward. Finally, the uniform translation of all particles along the orbit gives an effective rotation of the whole ring in the plane of the particle centers.

In addition to the translation  $dr$  in the plane of the triple ring, also the motion  $dz$  perpendicular to the ring has to be considered. Collectively, the particles move up and down, resulting in an oscillating up-and-down translation of the ring. Due to the broken symmetry caused by  $\cos\varphi(\theta)$ , the trajectory in  $z$ -direction is not reversible either. However, the vertical component  $z$  that is gained during  $d\theta > 0$  is reversed during  $d\theta < 0$ , and the ring gains no overall distance along  $z$ .

For a ring that is located on a surface, the translation  $r(t)$  has been obtained analogously (Fig. 3D). In this case, the factor  $c(\theta) = c_f(\theta) \cdot c_r(\theta)$  has been applied in Eq. 4a. The translational behavior differs qualitatively from the one in an isotropic medium if a value  $c_{r,2} < 0$  is applied, i.e. if the surface drag dominates over the effect of the dipole shift on the translation. Then, negative values of  $c_{r,2}$  reverse the sign of the displacements in sections III and IV. Thus, forth displacement takes place during II/III and back displacement occurs during I/IV (Fig. 3D). During I/II, where  $c_{r,1} > 0$  is effective, the translation  $r(t)$  looks similar to the one without surface. Further, since on the surface  $|c_1| > |c_2|$ ,  $dr(\theta_I) + dr(\theta_{II}) < dr(\theta_{III}) + dr(\theta_{IV})$  holds. Also in this scenario the integrated forth displacement  $r$  (facing the

non-magnetic side) is larger than the back displacement (magnetic side) during one field cycle. In the example presented in Fig. 3D, the ratio  $c_2/c_1 = -0.2$  has been applied. This ratio is also visible in the curve  $r(t)$  by the ratio between the amplitude during I/II and the one during III/IV.

The proposed concept of actuation is, of course, not limited to the triple cluster, which is, however, the smallest entity showing this effect. The concept can be applied to other clusters, too, as will be shown next by experimental studies.

### Actuated clusters of capped particles

The proposed actuation of interacting sd-particles under oscillating fields can indeed be found in an experimental system. We use particles with a hemispherical magnetic coating, so-called capped or Janus particles. Due to the hemispherical coating, the magnetic center of mass is shifted away from the particle center. Using a ferromagnetic coating with perpendicular magnetic anisotropy gives a dipole moment that points radially outwards [40]. For such a particle, the orientation of the dipole coincides with the Janus director, which is visualized by transmission light microscopy via the optical contrast between the transparent, uncoated and the in-transparent, coated hemisphere. After sedimentation on a substrate, these particles assemble in a great variety of open and compact two-dimensional structures with di-

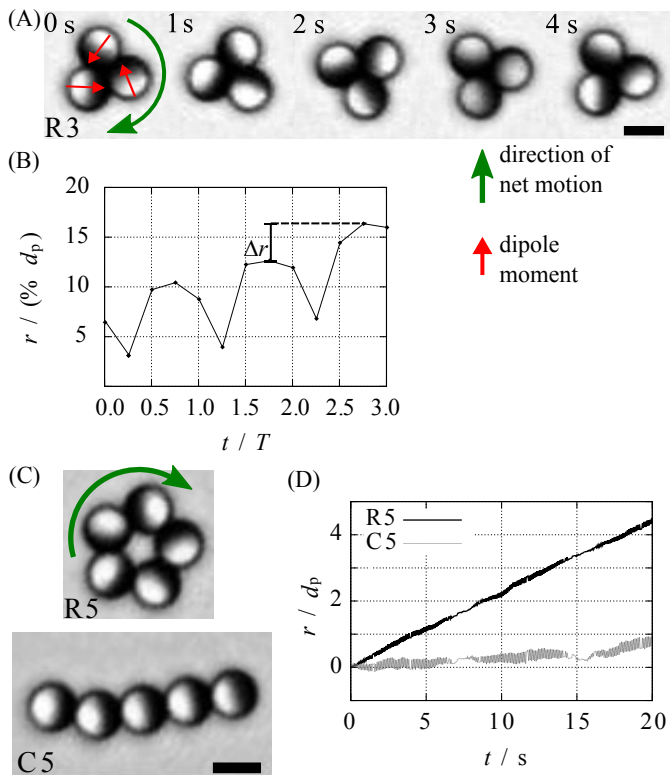


FIG. 4. Actuation of colloidal clusters. (A) Image sequence of the rotation of a self-assembled triple ring (R3) under an oscillating field. (B) Orbital translation  $r(t)$  of a capped particle in R3 for three periods  $T$  ( $B_0^z = 0.57$  mT,  $\omega_B/2\pi = 5$  Hz at 20 fps). (C) Microscopy images of a five-particle ring (R5) and a linear chain (C5) that form under weak oscillating fields. (D)  $r(t)$  of a particle in R5 and C5 ( $B_0^z = 1.22$  mT,  $\omega_B/2\pi = 10$  Hz). The superimposed beat results from the stroboscopic recording with a digital camera (20 fps). (Scale bars:  $5 \mu\text{m}$ )

verse magnetic order [41, 42]. In the following the behavior of selected structures under oscillating fields will be presented and compared.

Spontaneously, the capped particles self-assemble into triple rings (R3). If such a ring is exposed to oscillating fields  $B^z$ , one can indeed observe that it rotates (Fig. 4A). The uncapped, non-magnetic hemisphere always faces towards the direction of net rotation of the ring, as expected from the simulations presented above. The translations  $r(t)$  of the particles with diameter  $d_p = 4.54 \mu\text{m}$  have been accessed quantitatively by image analysis. In Fig. 4B,  $r(t)$  is plotted over three movement cycles with four data points each. The net translation can be concluded from the averaged slope of the curve. The relative increase  $\Delta r/d_p$  per cycle for the capped particles is in the range of a few %. The larger value of  $\Delta r/d_p$  in comparison with that obtained for sd-particles (Fig. 3B) results from the broad magnetization distribution of the capped particles, which leads to a slight modification of

the interaction potential that is assumed between particles with one shifted point dipole each [41]. Qualitatively, the curve in Fig. 4B looks similar to the one proposed for particles in a ring on the substrate (Fig. 3D). Both exhibit a motion sequence of fast forth, slow forth, slow back, and fast back translation, where the speed corresponds to the local slope of the curve  $r(t)$ . In analogy to the simulation, the ratio between the amplitudes during the section of the slow and fast translation gives a measure for the ratio between the conversion factors  $c_1$  and  $c_2$ . The amplitudes in the experimental curve (Fig. 4B) suggest that  $c_2/c_1 \approx -0.2$ . We propose that only the distance between particles and substrate determines  $c_2/c_1$ . The actuation of particles with various surface coatings on the magnetic hemisphere has shown that the two chemically different surfaces of the particles have no influence on the propulsion efficiency.

Next, we have tested whether the actuation concept also holds for other clusters. Capped particles (and also sd-particles) do not form larger rings spontaneously due to the magnetic asymmetry. However, we have shown earlier that closed rings and linear chains (R5 and C5 in Fig. 4C) can form if weak, low-frequency oscillating fields are applied [43]. The presence of these clusters is, thus, linked directly to any motion of these clusters under oscillating fields. We have observed that R5 rotates in the image plane, leading to a significant slope in  $r(t)$  (Fig. 4D). This is in agreement with the above discussion. In contrast, under the same environmental conditions, chains (C5) only perform periodic back and forth displacement along the chain direction with almost no net translation. We have found previously that the loop trajectory, which breaks time-reversal symmetry, only exists for non-collinear dipolar particles with non-zero shift [41]. Simulations of sd-particles in a linear chain have shown that under oscillating fields their dipoles obtain a head-to-tail orientation where they perform only reciprocal oscillations  $\theta(t)$  without variation in  $\varphi$ . This implies that collinear sd-particles under oscillating fields do not exhibit loop-trajectories, and, thus, they cannot translate. The small, but yet visible, slope in the trajectory of C5 (Fig. 4D) implies that the particles in C5 are not perfectly collinear at all times, resulting in a weak translation along the chain direction. This might be caused by thermally induced bending (deformation) of the chain.

So far, the actuation of interacting sd-particles has been demonstrated for ring clusters to take advantage of symmetric boundary conditions. Of course, the presented concept also holds if the assembled cluster is not rotationally symmetric. Since the motion of a cluster arises from the sum of the displacements  $dr$  of the constituting particles, the lack of rotational symmetry can result in more diverse motion. As an example, two compact clusters consisting of five particles (Fig. 5A, B) have been actuated by oscillating fields. These stable clusters, which have formed by self-assembly, exhibit the same

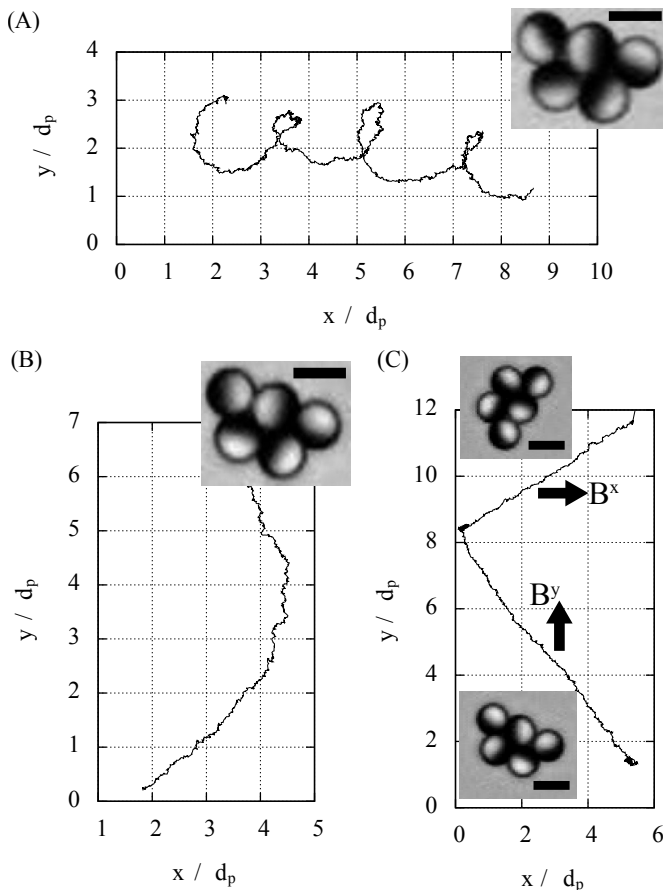


FIG. 5. Trajectory of the center of mass of two compact clusters (insets) (A, B) under an oscillating field with  $B^z = 0.53$  mT,  $\omega_B/2\pi = 5$  Hz (A: 88 s; B: 251 s) and (C) under an oscillating field ( $B^z = 1.13$  mT,  $\omega_B/2\pi = 20$  Hz) and a constant in-plane field ( $B^{x/y} = 0.03$  mT). The orientation of  $B^{x/y}$  is switched from the  $y$ -axis to the  $x$ -axis during the recording, leading to a change of the translation direction. (Scale bars:  $5 \mu\text{m}$ )

spatial shape but slightly different magnetic configurations. Specifically, they differ in the azimuthal orientation of only one particle (most left one in the insets in Fig. 5) while all other four particles are similar. Interestingly, this small difference in the magnetic configuration leads to a drastic difference in the trajectory of the clusters when actuated by oscillating fields (Fig. 5 A, B). One of the clusters (a) performs a screw-like motion while the other (b) exhibits an almost linear path. This can be understood when considering that each particle in a cluster contributes to the overall translation with a component  $dr$  that points along its dipole moment, i.e. the in-plane cap orientation. In cluster (a) the dipole vectors of the particles form a bent ring, which leads to the observed helical motion. In cluster (b), the vectorial sum of the cap orientations gives a significant net magnetic moment, leading to directed translation of the cluster.

The net moment additionally can be used to orient the

cluster in weak fields parallel to the cluster plane. This enables a control over the translation direction (Fig. 5 C). After orienting the cluster along a parallel field, it performs directed translation under an additional oscillating field. Switching the in-plane field orientation by  $90^\circ$  results in a change of the translation direction. A noteworthy feature in the example presented in Fig. 5 C is that the translation path is not parallel to the direction of the applied field, because the net magnetic orientation of this cluster does not coincide with its effective translation direction.

## DISCUSSION

In a highly viscous environment, microscopic objects can be actuated by an oscillating field only if they exhibit two addressable coordinates of motion. This is necessary in order to break time-reversal symmetry in the absence of inertia. Here, we have proposed that actuation of structurally non-deforming microscopic objects under oscillating fields is possible under certain conditions without the need for anisotropic drag. The concept requires a multi-component object (cluster), where the interaction between the oscillating components activates a coordinate of motion that is different from the coordinate along which the oscillating field acts. In the example presented here, the components are magnetic spheres. They can rotate in response to the external field, and, additionally, in response to the interaction with their magnetic neighbors. Time-reversal symmetry under oscillating fields is broken if the particles exhibit an anisotropic magnetization distribution and if they do not form a dipolar head-to-tail chain. Then, the interparticle interaction causes a torsional oscillation perpendicular to the field direction, leading to non-reciprocal motion. This actuation concept does not require an anisotropic environment. As explained here for a ring cluster, the presence of anisotropic drag close to a surface only modifies the motion. We propose that this actuation concept can be generalized to other objects that consist of particles with anisotropic interaction comparable to that caused by the magnetic shift [44–46].

The benefit of this approach lies in the variability of the following three features. First and most striking, the overall translation pattern can take different paths depending on the respective magnetic configuration of a cluster. Second, the translation direction can be controlled. Third, from the equation of motion (Eq. 6) it can be deduced that the speed of motion is adjustable by varying the amplitude of the oscillating field. The path of a cluster arises from the sum of the contributions of each constituting particle.

Ring clusters perform rotation under oscillating fields due to their rotational symmetry. Other, asymmetric clusters perform directed translation as demonstrated by

magnetically capped particles. The motion crucially depends on the position and orientation of each constituting particle. The modification of only one particle orientation drastically influences the translation path. This suggests that by proper assembly of a cluster two-dimensional rotation and translation as well as any combination of both can be realized. To predict the translation path of a cluster other than a ring cluster full numerical simulations are required. For those, the shape asymmetry of a cluster additionally requires to include hydrodynamic drag [47, 48], providing a complex problem on its own. Since a translating cluster exhibits a residual magnetic moment, the orientation of the whole cluster can be controlled by a weak, constant field. A superimposed oscillating field then leads to orientation-controlled directed translation. Thus, the actuation with a single field component advantageously gives two remaining field components free for controlling the translation direction.

From the presented concept, we derive that the field amplitude directly controls the actuation speed. The field amplitude is directly proportional to the angular velocity of the particles, which controls the size of the oscillation amplitude  $\theta_A$  as the integration bounds of Eq. 4. Therefore, the field amplitude determines the displacement  $\Delta r$  per movement cycle.

In conclusion, the presented results show that anisotropic interactions between the rotatable components of an object enable actuation in highly viscous media. This provides a promising alternative to anisotropic drag as the commonly used actuation principle. Based on the simplicity of the applied field pattern that drives the motion, the question remains whether similar motion patterns can be found in animate systems. In addition to anisotropic interaction potentials, also entropic interactions between (plentiful available) components with anisotropic shape [49] might provide comparable propulsion mechanisms based on the idea of non-reciprocal oscillation.

Financial support by the German Research Foundation (DFG, Grant Nos. ER 341/9-1, AL618/11-1, and FOR 1713 GE 1202/9-1) is gratefully acknowledged. We are grateful to Bjoergvin Hjörvarsson for pointing to the locomotion process in the microscopy recordings. We thank Henrique Moyses and Jeremy Palacci for fruitful discussions.

## APPENDIX

### Analytic calculation of the infinitesimal displacement

A dipolar sphere that is exerted to a magnetic torque rotates around its magnetic center. If the magnetic center is shifted away by  $\xi \frac{d_p}{2}$  from the geometric center, as given for sd-particles, then the rotation leads to a displacement of the sphere center. The path of motion is an arc

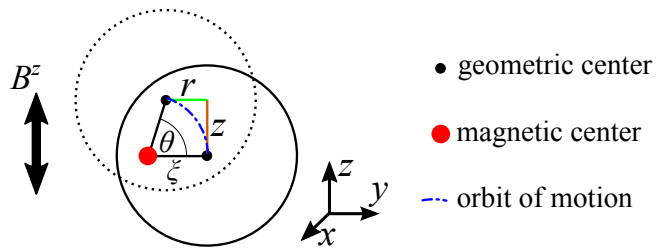


FIG. 6. Sketch of a sphere before (solid circle) and after (dotted circle) rotation by  $\theta$  around the magnetic center that is shifted by  $\xi$ . The center of the sphere moves by  $r = \sqrt{x^2 + y^2}$  ( $\perp B^z$ ) and  $z$  ( $\parallel B^z$ ).

(Fig. S1) with a radius determined by the magnetic shift. Here, the displacement of an sd-particle that rotates in response to an external field pointing along the  $z$ -axis is considered. The displacement of sd-particles caused by the rotation by an angle  $\theta$  in an isotropic medium can be expressed analytically. When rotating about the magnetic center (dipole position), the ideal displacements perpendicular ( $r$ ) and parallel ( $z$ ) to an oscillating field  $B^z$  are given by

$$r = \xi(\cos \theta - 1) \frac{d_p}{2}, \quad z = \xi \sin \theta \frac{d_p}{2}. \quad (3)$$

In viscous medium, translational drag reduces this displacement, which can be regarded as an effective shift of the rotation axis away from the magnetic center towards the particle center. In an isotropic medium, viscous drag leads to a constant reduction factor. It can, thus, be disregarded here for a qualitative description of the actuation process where only anisotropic drag is relevant. From the differentiation of  $r$  and  $z$  with respect to  $\theta$  one obtains

$$dr = d\theta c(\theta) \xi(-\sin \theta) \frac{d_p}{2}, \quad dz = d\theta c(\theta) \xi \cos \theta \frac{d_p}{2}. \quad (4)$$

Sources of anisotropic friction that hinder or enhance this displacement are incorporated by the additional term  $c(\theta)$ .

### Numerical Methods

The rotational motion of interacting sd-particles in a ring cluster exposed to an oscillating field  $\mathbf{B}^z = B_0^z \sin(\omega t)$  has been calculated by numerically solving the equation of rotation. In this simulation, the particles are spatially fixed at their center. This assumption is reasonable when studying exclusively the rotation of the particles in the reference system of a cluster that does not change its spatial shape. Assuming sd-particles with dipole moment  $\mathbf{m}$  (unit vector  $\hat{\mathbf{m}}$ ) and stray field  $\mathbf{B}^p$ , the equation of rotation is obtained by balancing the rotational drag,  $\tau^d$ , with the torques between the

sd-particles and between sd-particles and the field,  $\tau^B$ . Inertial forces have been neglected taking into account the highly viscous environment. Note that due to the dipole shift, besides the aligning torque  $\tau^P = \mathbf{m} \times \mathbf{B}^P$ , also the gradient force  $(\mathbf{m} \cdot \nabla)\mathbf{B}^P$  between the sd-particles is relevant. The latter converts into an effective torque,  $\tau^F$ , such that the equation of rotation is given by

$$\tau^d = \tau^P + \tau^F + \tau^B \quad (5)$$

$$f_r \dot{\Theta}(t) = \mathbf{m} \times \mathbf{B}^P + \xi \hat{\mathbf{m}} \times ((\mathbf{m} \cdot \nabla)\mathbf{B}^P) + \mathbf{m} \times \mathbf{B}^z \quad (6)$$

$\dot{\Theta}$  is the angular velocity of an object with rotational friction coefficient  $f_r$  and orientation  $\Theta = (\theta, \varphi)$  (Fig. 3 A). An ensemble of  $n$  particles gives a system of  $n$  coupled equations of rotation (Eq. 6), which are solved iteratively in a self-consistent cycle. From the state at time  $t$ , the magnetic moment  $\mathbf{m}_i$  of particle  $i$  at time step  $t + 1$  is obtained by

$$\hat{\mathbf{m}}_i^{(t+1)} = \text{norm} \left[ \hat{\mathbf{m}}_i^{(t)} + \frac{1}{f_r} (\tau^P + \tau^F + m_i \times (B_0^z \cos(\omega t))) \right] \quad (7)$$

The function 'norm[.]' scales the updated magnetic moments  $\mathbf{m}^{(t+1)}$  to retain the initial magnitude  $m$  of the dipoles. In the calculation, a rotational friction coefficient of  $f_r = 100 \frac{\mu_0 m^2}{32\pi r_p^3}$  has been applied. It has the dimension of energy since the numerical time steps  $\Delta t = (t + 1) - t$  are dimensionless and set to 1. The angular frequency  $\omega$  is also a dimensionless quantity and is set to 0.05.

### Calculation of the time-dependent translation

The time-dependent translation  $r(t)$  of sd-particles along the orbit of the triple ring can be calculated by integrating Eq. 4 after inserting analytic expressions of  $\varphi(t)$ ,  $\theta(t)$ , and  $c(\theta) = \cos(\varphi(\theta(t)))$ . The expressions are obtained by fitting the steady-state trajectory  $\varphi(\theta)$  (Fig. 3 B in the main article) to a Lissajous curve. The fitting curve has the form

$$\varphi(\theta) = \varphi_A \sin \left( 2 \arcsin \frac{\pm \theta}{\theta_A} + p \right) + n \quad (8)$$

with the azimuthal and the radial amplitudes  $\varphi_A$  and  $\theta_A$ , the phase shift  $p$  between  $\varphi$  and  $\theta$  and the offset  $n$  of the angle  $\varphi$  caused by the dipole shift. The sign  $\pm$  accounts for the fact that  $\varphi(\theta)$  is a multivalued function.  $\varphi$  and  $\theta$  perform harmonic oscillations with a frequency ratio of  $\omega_\varphi/\omega_\theta = 2$ .  $\omega_\theta$  equals the actuation frequency  $\omega_B$  of the external field. With the fit parameters  $\varphi_A, \theta_A, p, n$ , the time-dependent oscillations can be expressed by  $\varphi(t) = \varphi_A \sin(2\omega_B t + p) + n$  and  $\theta(t) = \theta_A \sin(\omega_B t)$ . From the differentiation  $\frac{d\theta(t)}{dt}$  we obtain the substitution for the integration variable as  $d\theta = dt \theta_A \omega_B \cos(\omega_B t)$ . The time-dependent translation is then given by the integration

$r(t') = \int_0^{t'} dr(t)$ . For particles in a ring that is located on a surface, the translation can be calculated analogously by taking into account that  $c(\theta) = \cos \varphi(\theta(t)) \cdot c_f(\theta)$ .

### Experimental Details

The particle preparation and experimental setup has been described in detail in reference [43]. In short, silica spheres with a radius of  $r_p = (2.27 \pm 0.23) \mu\text{m}$  have been coated on one hemisphere with a magnetic thin film of  $[\text{Co}(0.28 \text{ nm})/\text{Pd}(0.9 \text{ nm})]_8$  [40]. The film exhibits perpendicular magnetic anisotropy. After magnetic saturation, this leads to the dipole-like stray field when deposited on spheres. A suspension of such particles in distilled water is studied via transmission light microscopy. Due to the density mismatch the particles sediment on the ground of the sample cell, providing a two-dimensional particle system. An electromagnetic coil is mounted above the sample cell, providing perpendicular low-frequency fields. An additional set of two pairs of coils attached beneath the sample provide constant fields to orient translating clusters. The recordings of the moving clusters have been analyzed by optical image analysis using the open-source software ImageJ and the included plugin 'particle analysis'.

- 
- [1] Purcell EM (1977) Life at low Reynolds number. *Am J Phys* 45(1):3.
  - [2] Lauga E, Powers TR (2009) The hydrodynamics of swimming microorganisms. *Rep Prog Phys* 72(9):096601.
  - [3] Bechinger C, et al. (2016) Active Brownian particles in complex and crowded environments. arXiv:1602.00081.
  - [4] Elgeti J, Winkler RG, Gompper G (2015) Physics of microswimmers - single particle motion and collective behavior: a review. *Rep Prog Phys* 78(5):056601.
  - [5] Golestanian R, Yeomans JM, Uchida N (2011) Hydrodynamic synchronization at low Reynolds number. *Soft Matter* 7(7):3074-3082.
  - [6] Dunkel J, Zaid IM (2009) Noisy swimming at low Reynolds numbers. *Phys Rev E* 80(2):021903.
  - [7] Fletcher DA, Geissler PL (2009) Active biological materials. *Annu Rev Phys Chem* 60:469-486.
  - [8] Stone HA, Samuel ADT (1996) Propulsion of microorganisms by surface distortions. *Phys Rev Lett* 77(19):4102-4104.
  - [9] Arroyo M, Heltai L, Millan D, DeSimone A (2012) Reverse engineering the euglenoid movement. *Proc Natl Acad Sci USA* 109(44):17874-17879.
  - [10] Tam D, Hosoi AE (2011) Optimal feeding and swimming gaits of biflagellated organisms. *Proc Natl Acad Sci USA* 108(3):1001-1006.
  - [11] Goldstein RE (2015) Green algae as model organisms for biological fluid dynamics. *Annu Rev Fluid Mech* 47:343-375.
  - [12] Wan KY, Goldstein RE (2016) Coordinated beating of algal flagella is mediated by basal coupling. *Proc Natl*

- Acad Sci USA* 113(20):E2784-E2793.
- [13] Elgeti J, Gompper G (2013) Emergence of metachronal waves in cilia arrays. *Proc Natl Acad Sci USA* 110(12):4470-4475.
- [14] Jung I, Powers TR, Valles JM (2014) Evidence for two extremes of ciliary motor response in a single swimming microorganism. *Biophys J* 106(1):106-113.
- [15] Abbott JJ, et al. (2009) How should microrobots swim? *Int J Robot Res* 28(11-12):1434-1447.
- [16] Rao KJ, et al. (2015) A force to be reckoned with: A review of synthetic microswimmers powered by ultrasound. *Small* 11(24):2836-2846.
- [17] Zottl A, Stark H (2016) Emergent behavior in active colloids. *J Phys Condens Matter* 28(25):253001.
- [18] Najafi A, Golestanian R (2004) Simple swimmer at low Reynolds number: Three linked spheres. *Phys Rev E* 69(6):062901.
- [19] Palagi S, et al. (2016) Structured light enables biomimetic swimming and versatile locomotion of photoresponsive soft microrobots. *Nat Mater* 15(6):647653.
- [20] Palacci J, Sacanna S, Steinberg AP, Pine DJ, Chaikin PM (2013) Living crystals of light-activated colloidal surfers. *Science* 339(6122):936-940.
- [21] Chalupniak A, Morales-Narvaez E, Merkoci A (2015) Micro and nanomotors in diagnostics. *Adv Drug Deliver Rev* 95:104-116.
- [22] Erbe A, Zientara M, Baraban L, Kreidler C, Leiderer P (2008) Various driving mechanisms for generating motion of colloidal particles. *J Phys Condens Matter* 20(40):404215.
- [23] Vach PJ, Faivre D (2015) The triathlon of magnetic actuation: Rolling, propelling, swimming with a single magnetic material. *Sci Rep* 5:09364.
- [24] Fischer P, Ghosh A (2011) Magnetically actuated propulsion at low Reynolds numbers: towards nanoscale control. *Nanoscale* 3(2):557-563.
- [25] Khaderi SN, den Toonder JMJ, Onck PR (2015) Magnetic artificial cilia for microfluidic propulsion. *Adv Appl Mech* 48:1-78.
- [26] Martinez-Pedrero F, Tierno P (2015) Magnetic propulsion of self-assembled colloidal carpets: Efficient cargo transport via a conveyor-belt effect. *Phys Rev Appl* 3(5):051003.
- [27] Tierno P (2014) Recent advances in anisotropic magnetic colloids: realization, assembly and applications. *Phys Chem Chem Phys* 16(43):23515.
- [28] Zhang L, et al. (2009) Characterizing the swimming properties of artificial bacterial flagella. *Nano Lett* 9(10):3663-3667.
- [29] Casic N, et al. (2013) Propulsion efficiency of a dynamic self-assembled helical ribbon. *Phys Rev Lett* 110(16):168302.
- [30] Ghosh A, Fischer P (2009) Controlled propulsion of artificial magnetic nanostructured propellers. *Nano Lett* 9(6):2243-2245.
- [31] Goldman AJ, Cox RG, Brenner H (1967) Slow viscous motion of a sphere parallel to a plane wall. I. Motion through a quiescent fluid. *Chem Eng Sci* 22(4):637.
- [32] Tierno P, Golestanian R, Pagonabarraga I, Sagues F (2008) Controlled swimming in confined fluids of magnetically actuated colloidal rotors. *Phys Rev Lett* 101(21):218304.
- [33] Zhang L, et al. (2010) Controlled propulsion and cargo transport of rotating nickel nanowires near a patterned solid surface. *ACS Nano* 4(10):6228-6234.
- [34] Tierno P, Sagues F (2012) Steering trajectories in magnetically actuated colloidal propellers. *Eur Phys J E* 35(8):71.
- [35] Dreyfus R, et al. (2005) Microscopic artificial swimmers. *Nature* 437(7060):862-865.
- [36] Benkoski JJ, et al. (2011) Dipolar organization and magnetic actuation of flagella-like nanoparticle assemblies. *J Mater Chem* 21(20):7314-7325.
- [37] Gauger E, Stark H (2006) Numerical study of a microscopic artificial swimmer. *Phys Rev E* 74(2):021907.
- [38] Trouilloud R, Yu TS, Hosoi AE, Lauga E (2008) Soft swimming: Exploiting deformable interfaces for low Reynolds number locomotion. *Phys Rev Lett* 101(4):048102.
- [39] Chen CH, Abate AR, Lee DY, Terentjev EM, Weitz DA (2009) Microfluidic assembly of magnetic hydrogel particles with uniformly anisotropic structure. *Adv Mater* 21(31):32013204.
- [40] Albrecht M, et al. (2005) Magnetic multilayers on nanospheres. *Nat Mater* 4(3):203-206.
- [41] Steinbach G, et al. (2016) Bistable self-assembly in homogeneous colloidal systems for flexible modular architectures. *Soft Matter* 12(10):2737-2743.
- [42] Baraban L, et al. (2008) Frustration-induced magic number clusters of colloidal magnetic particles. *Phys Rev E* 77(3):031407.
- [43] Steinbach G, Gemming S, Erbe A (2016) Non-equilibrium dynamics of magnetically anisotropic particles under oscillating fields. *Eur Phys J E*.
- [44] Yener AB, Klapp SHL (2016) Self-assembly of three-dimensional ensembles of magnetic particles with laterally shifted dipoles. *Soft Matter* 12(7):2066-2075.
- [45] Sacanna S, Rossi L, Pine DJ (2012) Magnetic click colloidal assembly. *J Am Chem Soc* 134(14):6112-6115.
- [46] Abrikosov AI, Sacanna S, Philipse AP, Linse P (2013) Self-assembly of spherical colloidal particles with off-centered magnetic dipoles. *Soft Matter* 9(37):8904-8913.
- [47] Kümmel F, et al. (2013) Circular motion of asymmetric self-propelling particles. *Phys Rev Lett* 110(19):198302.
- [48] Wensink HH, Kantsler V, Goldstein RE, Dunkel J (2014) Controlling active self-assembly through broken particle-shape symmetry. *Phys Rev E* 89:010302.
- [49] Glotzer SC, Solomon MJ (2007) Anisotropy of building blocks and their assembly into complex structures. *Nat Mater* 6(8):557-562.